Restoration of Mitochondrial Integrity, Telomere Length, and Sensitivity to Oxidation by In Vitro Culture of Fuchs' Endothelial Corneal Dystrophy Cells

Sébastien P. Gendron,[1,2] Mathieu Thériault,[1,2] Stéphanie Proulx,[1–3] Isabelle Brunette,[4,5] and Patrick J. Rochette[1–3]

[1]Axe Médecine Régénératrice, Centre de Recherche du CHU de Québec-Université Laval, Hôpital du Saint-Sacrement, Québec, Québec, Canada
[2]Centre de Recherche en Organogénèse Expérimentale de l'Université Laval/LOEX, Université Laval, Québec, Québec, Canada
[3]Département d'Ophtalmologie et ORL-Chirurgie cervico-faciale, Université Laval, Québec, Québec, Canada
[4]Maisonneuve-Rosemont Hospital Research Center, Montreal, Québec, Canada
[5]Department of Ophthalmology, University of Montreal, Montreal, Québec, Canada

Correspondence: Patrick J. Rochette, Axe Médecine Régénératrice, Centre de Recherche du CHU de Québec-Université Laval, Hôpital du Saint-Sacrement, Québec, Québec, Canada;
Patrick.rochette@orlo.ulaval.ca.

Submitted: August 17, 2016
Accepted: September 29, 2016

Citation: Gendron SP, Thériault M, Proulx S, Brunette I, Rochette PJ. Restoration of mitochondrial integrity, telomere length, and sensitivity to oxidation by in vitro culture of Fuchs' endothelial corneal dystrophy cells. *Invest Ophthalmol Vis Sci*. 2016;57:5926–5934. DOI:10.1167/iovs.16-20551

Purpose. Fuchs' endothelial corneal dystrophy (FECD), a degenerative disease of the corneal endothelium that leads to vision loss, is a leading cause of corneal transplantation. The cause of this disease is still unknown, but the implication of oxidative stress is strongly suggested. In this study, we analyzed the impact of FECD on mitochondrial DNA (mtDNA) integrity and telomere length, both of which are affected by the oxidative status of the cell.

Methods. We compared the levels of total mtDNA, mtDNA common deletion (4977 bp), and relative telomere length in the corneal endothelial cells of fresh Descemet's membrane-endothelium explants and cultured cells from healthy and late stage FECD subjects. Oxidant-antioxidant gene expression and sensitivity to ultraviolet A (UVA)- and H_2O_2-induced cell death were assessed in cultured cells.

Results. Our results revealed increased mtDNA levels and telomere shortening in FECD explants. We also found that cell culture restores a normal phenotype in terms of mtDNA levels, telomere length, oxidant-antioxidant gene expression balance, and sensitivity to oxidative stress-induced cell death in the FECD cells compared with the healthy cells.

Conclusions. Taken together, these results bring new evidence of the implication of oxidative stress in FECD. They also show that FECD does not evenly affect the integrity of corneal endothelial cells and that cell culture can rehabilitate the molecular phenotypes related to oxidative stress by selecting the more functional FECD cells.

Keywords: corneal endothelial cells, Fuchs' endothelial corneal dystrophy, mitochondria, oxidation, telomere

The posterior layer of the human cornea, the corneal endothelium, is crucial for corneal transparency, because it controls corneal deturgescence. Fuchs' endothelial corneal dystrophy (FECD) is a degenerative disease of the corneal endothelium. The prevalence of FECD in the United States is estimated at 897 per million individuals, and the symptoms usually appear after 60 years of age.[1] FECD is typically characterized by an abnormal deposition of extracellular matrix on the posterior aspect of Descemet's membrane, generating excrescences called guttae. The progressive enlargement of these guttae is associated with a progressive and irreversible loss of endothelial cells. This leads to corneal edema, which, if left untreated, results in painful bullous keratopathy, scarring, and blindness.[2,3] The only treatment currently available to restore sight is corneal endothelial transplantation.[2] FECD is the leading indication for corneal endothelial transplantation and was responsible for 53.4% of the 28,064 endothelial keratoplasties performed in the United States in 2014. The cause of the disease is believed to involve hereditary and hormonal and environmental factors.[4]

The corneal endothelium is continuously exposed to endogenous and exogenous oxidative stress. Its deturgescence activity induces a high aerobic metabolism. To compensate for the leakage of fluid from the aqueous humor to the corneal stroma, endothelial basolateral Na^+/K^+-ATPases and Na^+/HCO_3^- co-transporters actively transport ions, generating an osmotic gradient and thus a water flux out of the cell to the anterior chamber.[5] This high aerobic metabolism leads to endogenous oxidation and generation of reactive oxygen species (ROS). The cornea is also constantly exposed to sunlight ultraviolet (UV) radiation, the UV A portion of which reaches the corneal endothelium.[6,7] UVA light is well described as an exogenous oxidizer that generates ROS.[8] Together, the high aerobic metabolism, the lifetime exposure to toxic sunlight, and the fact that the corneal endothelial cells in vivo are arrested in the G_1 phase of the cycle (i.e., nonmitotic cells) make the corneal endothelium prone to oxidative stress.[9]

Generation of ROS from both endogenous and exogenous sources can oxidize DNA and induce the mutagenic 8-hydroxy-2′-deoxyguanosine (8-oxoG). Accumulation of 8-oxoG was

Investigative Ophthalmology & Visual Science

recently described in FECD corneal endothelial cells, mostly at the level of mitochondrial DNA (mtDNA).[3,10] mtDNA is highly susceptible to oxidative damage because of its direct exposure to the ROS-generating respiratory chain and its lack of histone protection.[10,11] Damage to the mtDNA can cause loss of integrity of the inner mitochondrial membrane potential, apoptosis, and accumulation mtDNA deletions, leading to dysfunctional synthesis of mitochondrial proteins.[12–14] Telomeric DNA is also sensitive to oxidative damage, which induces telomeric shortening, acceleration of cellular senescence, and impaired cell function.[15,16,17]

Several observations indicate that FECD cells are poorly protected against oxidative stress. (1) The DJ-1 protein, known to protect against oxidative damage, is downregulated in FECD. This results in an impaired nuclear factor erythroid 2-related factor 2 (Nrf2) nuclear translocation.[18] Nrf2 is a transcription factor that regulates the expression of antioxidant proteins. The impaired translocation of Nrf2 sensitizes the corneal endothelial cell to UVA light by decreasing the expression of antioxidant genes, increasing oxidative damage, and activating p53-dependant apoptosis.[9,19] (2) Transcriptome analyses have shown that mitochondrial antioxidant genes, such as superoxide dismutase 2 (SOD2) and Prx3, are downregulated in FECD.[20] (3) Oxidative stress involving lipid peroxidation, advanced glycation end-products, and other ROS was shown to be implicated in FECD.[21,22] (4) An imbalance in oxidant-antioxidant toward a pro-oxidant state was documented in FECD in several studies.[3,10,23]

Our group recently showed that FECD endothelial cells could be successfully cultured without transduction. We also demonstrated that the diseased endothelial cells of clinically decompensated FECD corneas, when cultured and seeded on a devitalized stromal carrier and transplanted into the living animal eye, can recover active pump function and restore corneal transparency for at least 7 days after transplantation.[24] The partial recovery in culture of these end-stage FECD endothelial cells harvested from the central and most diseased part of the cornea has opened the door to a new perspective, which is herein analyzed from an "oxidation standpoint."

The goal of this study was to investigate the effect of cell culture on the oxidative imbalance documented in FECD corneal endothelial cells. More specifically, using specimens from FECD and normal subjects, we compared the corneal endothelial cells of fresh corneal endothelial explants with endothelial cells in culture, looking for differences in mitochondrial DNA levels, mtDNA integrity, telomere shortening, sensitivity to oxidative stress-induced cell death, and oxidant-antioxidant gene expression. Increased mtDNA levels and telomere shortening were observed in fresh FECD explants but not in cultured FECD cells. On the other hand, mitochondrial integrity, oxidant-antioxidant gene expression, and sensitivity to oxidative stress-induced cell death were identical in cultured FECD and healthy endothelial cells. Furthermore, restoration of a normal telomere length in culture was not associated with the reactivation of telomerase activity, suggesting that the normal phenotypes found in cultured FECD cells would result from the selection of the less affected FECD cells.

Materials and Methods

Mitochondrial levels, mtDNA integrity, telomere shortening, oxidant-antioxidant gene expression, and sensitivity to oxidative stress-induced cell death were investigated in healthy and FECD explants and cultured cells. All experiments performed in this study were conducted in accordance with the Declaration of Helsinki, and the research protocol received approval by the Maisonneuve-Rosemont Hospital and the CHU de Québec-Université Laval institutional ethics committees. Corneal endothelium and Descemet's membrane specimens were collected from 21 consenting patients (60–83 years of age; mean ± SD 72 ± 7 years of age) with late-stage FECD at the time of their corneal transplantation.[25] Twenty-four healthy human corneas (50–82 years of age; mean ± SD 65 ± 9 years of age) unsuitable for transplantation were obtained from our local eye bank (Banque d'Yeux du Centre universitaire d'ophtalmologie).

Cell Culture

Healthy Corneal Endothelial Cells. Healthy corneas were obtained within 48 hours of death. Corneas were kept in Optisol-GS corneal storage medium (Bausch & Lomb, Rochester, NY, USA) at 4°C until isolated from corneal endothelial cells.[26] Descemet's membrane was peeled from the corneas and incubated overnight in growth medium at 37°C and 8% CO_2. Treatment with 0.02% ethylene-diamine-tetra-acetic acid (Sigma Life Science, St. Louis, MO, USA) for 20 to 45 minutes and gentle up and down agitation of the pipet were used to detach the cells from the Descemet's membrane. Loose cells were then seeded in culture dishes covered with FNC coating mix (Athena Enzyme Systems, Baltimore, MD, USA) in OptiMem-I (Invitrogen, Burlington, ON, Canada) culture medium supplemented with 8% fetal bovine serum (HyClone, Logan, UT, USA), 5 ng/mL human epidermal growth factor (Austral Biologicals, San Ramon, CA, USA), 20 ng/mL nerve growth factor (Biomedical Technologies, Stoughton, MA, USA), 100 μg/mL bovine pituitary extract (Biomedical Technologies), 20 μg/mL ascorbic acid (Sigma), 0.08 % chondroitin sulfate (Sigma), 25 μg/mL gentamicin sulfate (Schering, Pointe Claire, QC, Canada), and 100 IU/mL penicillin G (Sigma).[27] For gene profiling analyses, cells were grown and cultured for 24 days post confluence, with the addition of hydrocortisone (0.4 μg/ml; Calbiochem, Etobicoke, ON, Canada) during the last 7 days of culture. Hydrocortisone is used to improve the maturation of corneal endothelial cells.

FECD Corneal Endothelial Cells. Endothelial cells from the surgical specimens were isolated and cultured following the same protocols as for healthy cells.

Corneal Stromal Fibroblasts and HT1080. Corneal stromal fibroblasts from a 68-year-old donor and fibrosarcoma cells (HT1080) were cultured to full confluence in Dulbecco's modified Eagle medium (Wisent, St-Bruno, Quebec, Canada) with 10% fetal bovine serum (Wisent) and 1% penicillin/streptomycin (Wisent) at 37 °C, 5% CO_2. Healthy and FECD corneal endothelial cells were cultured up to passage 3. Age, sex and clinical diagnosis of all donors from whom corneal tissue was used in this study are listed in Table 1.

DNA Isolation

For the $mtDNA^{CD4977}$ and mtDNA levels and telomere length analyses, total DNA (mitochondrial and nuclear) from healthy and FECD corneal endothelial cells was purified using DNeasy blood and tissue kit (Qiagen, Toronto, ON, Canada) according to the manufacturer's protocol and with a RNase A treatment.

Analyses of $mtDNA^{CD4977}$ and mtDNA Levels by PCR

Levels of $mtDNA^{CD4977}$ and total mtDNA were measured using a Rotor-Gene Q real-time thermocycler (Qiagen). PCR amplifications were performed with previously published primers designed to amplify $mtDNA^{CD4977}$, total mtDNA, and genomic

Table 1. Classification of Age and Sex of Healthy and FECD Donors Used in This Study by Figure

Healthy (H) or FECD (F)	Age	Sex	Figure
F	60	Male	1A,1C,2A,2B
F	66	Female	1A,1B,1C,2A,2B
F	82	Female	1A,1B,1C,2A,2B
F	67	Male	1A
F	78	Male	1A
H	66	Female	1A,2A,2B
H	58	Male	1A,1C,2B
H	82	Female	1A,1C,2A,2B
H	72	Male	1A,1C,2A
H	77	Male	1A
H	66	Male	1A
F	83	Female	1A,2A
F	72	Male	2A
F	67	Male	1A,2A
F	66	Male	1A,2A
F	64	Male	1A
F	82	Male	1A
H	54	Male	1A,2A
H	69	Male	1A,2A
H	50	Female	1A
H	63	Male	1A,2A
H	77	Male	1A,2A
H	73	Male	1A,2A
H	50	Female	1A
H	82	Female	1B
H	66	Female	1B,1C
H	61	Female	1B
H	61	Female	1B
F	76	Male	1B
F	69	Male	1B
F	67	Male	2A
F	78	Male	2A
H	72	Female	2C
H	70	Female	2C
H	64	Female	2C
F	70	Male	2C
F	69	Male	2C
F	69	Male	2C
H	50	Female	3A,3B
H	59	Female	3A,3B
H	62	Female	3A,3b
H	72	Female	3A,3B
F	76	Male	3A,3B
F	79	Male	3A,3B
F	81	Male	3A,3B

DNA 18S.[14,28] Amplification was achieved using the primer sets shown in Table 2.

The mtDNA^{CD4977} primer set spans both sides of the common deletion. These primers, under our PCR conditions and a short primer extension time, allowed for DNA amplification of the deleted mtDNA molecules only. These primers are located in the cytochrome c oxidase II coding region, just outside the deleted region. The amplification was done with 10 ng of total DNA. Total mtDNA molecules were amplified with primers located in a region of the mitochondrial genome without reported deletion located in the 7S DNA coding region. A standard curve (5, 1, 0.1, 0.01, and 0.001 ng of total DNA/reaction) was performed using the total mtDNA primers. For each sample, the amplification level of mtDNA^{CD4977} primers was compared with the standard curve, and a ratio of mtDNA molecules containing the 4977-bp deletion-to-total mtDNA molecules (mtDNA^{CD4977}:mtDNA) ratio was derived. Samples with a cycle threshold (C_t) value over 35 amplification cycles were considered negative for the presence of mtDNA^{CD4977}. PCR reactions were performed in 20-μL reaction volumes containing 1× Brilliant III Ultra Fast SYBR Green Master Mix (Agilent Technologies, Santa Clara, CA, USA) and 500 nM of each primer. PCR conditions were 3 minutes at 95°C, followed by 40 cycles of 20 seconds at 95°C and 20 seconds at 60°C.

The mtDNA levels were measured with the previously described primer set and a primer set for nuclear genome located in the 18S ribosomal subunit DNA coding region, as shown in Table 2.[28] Amplification using the mtDNA primers was done with 0.25 ng of total DNA. A standard curve (5, 1, 0.5, 0.05, and 0.005 ng of total DNA/reaction) was performed with the 18S primers. For each sample, the amplification level of mtDNA primers was compared with the 18S DNA coding region standard curve, and a mtDNA molecules-to-18S coding region ratio (mtDNA:18S DNA) was derived. PCR conditions were the same as those described above for the mtDNA^{CD4977} primer set.

Mitochondrial Staining

Corneal endothelial cells (healthy and FECD) were cultured 24 days post confluence prior to mitochondrial staining, whereas central Descemet's membrane and attached endothelium explants were initially kept in Optisol-GS. Mitochondrial staining was performed using the Mitotracker Red CMXRos dye (Life Technologies, Burlington, ON, Canada) with minor modifications to the manufacturer's protocol. Briefly, samples were washed twice with prewarmed (37°C) OptiMem-I to remove serum oxidases from the culture medium and incubated in 250 nM (for cultured cells) or 40 nM (for explants) Mitotracker dye diluted in OptiMem-I for 40 minutes in the dark at 37°C with 8% CO_2. Samples were then washed twice with warm OptiMem-I (37°C), fixed in OptiMem-I containing 3.7% formaldehyde (Laboratoire Mat, Montreal, QC, Canada) in the dark at 37°C with 8% CO_2 for 15 minutes, and washed again twice with OptiMem-I. Next, samples were put on a microscope slide, mounted with SlowFade Gold antifade (Life Technologies), observed, and imaged.

Relative Telomere Length Analysis

Relative telomere length was assayed using a Rotor-Gene Q real-time thermocycler (Qiagen) with previously described primers.[29–31] Amplification was achieved using the primer sets and standards listed in Table 2. The telomere primer set allows amplification of telomeres of variable fragments over a size range because they can anneal at various distances apart on the telomeric repeats. The amplification was done with 0.5 ng of total DNA. A telomere standard oligomer of 14 repeats of the sequence 5′TTAGGG was used for the standard curve. A standard curve (60, 6, 0.6, 0.06, 0.006, and 0.0006 pg of total telomere standard/reaction) was performed with this oligomer with the addition of 2 pg of plasmid DNA without telomeric repeat (PCruzGFPL; Santa Cruz Biotechnology, Dallas, TX, USA) per reaction to allow efficient PCR reaction. For each sample, the amplification level of telomere primers was compared with the telomere standard curve, and a telomere repeat (T)-to-telomere standard (S) (T:S) ratio was derived.

The HBG primer set allows amplification of the hemoglobin gene, which is present in two copies in the human genome. Amplification using these primers was done with 0.5 ng of total DNA. An HBG standard oligomer corresponding to the coding DNA sequence of the gene was used for the standard curve. A

Table 2. Q-PCR Oligonucleotide Primers and Standards Used in This Study

Parameter	Primer	Amplicon Size, bp	Reference
18S ribosomal RNA coding region	F 5′-TAGAGGGACAAGTGGCGTTC R 5′-CGCTGAGCCAGTCAGTGT	104	28
mtDNA	F 5′-AATCAATTGGCGACCAATGG R 5′-CGCCTGGTTCTAGGAATAATGG	101	14
mtDNA^{CD4977}	F 5′-TATTAAACACAAACTACCACCTACC R 5′-GGCTCAGGCGTTTGTGTATGAT	132	14
HBG	F 5′-GCTTCTGACACAACTGTGTTCACTAGC R 5′-CACCAACTTCATCCACGTTCACC	120	29
Telomere	F 5′-GGTTTTTGAGGGTGAGGGTGAGGGTGAG R 5′-TCCCGACTATCCCTATCCCTACCCCTATC	variable	31
	Standard Oligomer		
Telomere standard	(TTAGGG)14	84	30
HBG standard	GCTTCTGACACAACTGTGTTCACTAGCAACCT CAAACAGACACCATGGTGCATCTGACTCCTG AGGAGAAGTCTGCCGTTACTGCCCTGTGGGG CAAGGTGAACGTGGATGAAGTTGGTG	120	NCBI GenBank identifier KP309825.1

standard curve (20, 2, 0.2, 0.02, 0.002, and 0.0002 pg of total HBG standard/reaction) was performed with this oligomer. For each sample, the amplification level of the HBG primers was compared with the HBG standard curve, and an "S" ratio of HBG copies-to-HBG standard (HBG copy: HBG standard) ratio was derived. A final ratio of T:S was derived to compare relative telomere length per cells. In all cases, PCR reactions were performed in 20 μL of reaction volumes containing 1× Brilliant III Ultra Fast SYBR Green Master Mix (Agilent Technologies) and 500 nM of each primer. PCR conditions were 3 minutes at 95°C, followed by 40 cycles of 20 seconds at 95°C and 60 seconds at 56°C.

Telomerase Repeat Amplification Protocol Assay

Corneal endothelial cells from healthy and FECD donors, a HT1080 fibrosarcoma telomerase-positive cell line and a 68-year-old telomerase-negative corneal keratocyte cell strain were cultured to full confluence. Total protein extracts were prepared, and telomerase catalytic activity was determined by using a telomerase repeat amplification protocol (TRAP) assay (TRAPeze telomerase detection kit; Chemicon International, Temecula, CA, USA) according to the manufacturer's protocol. The TRAP assay was performed using 0.6 μg of protein extract (equivalent to 1500 cells). The reaction mixture was incubated at 94°C for 30 seconds, 59°C for 30 seconds, and 72°C for 1 minute for 30 cycles on a thermocycler. The amplified products were resolved on a 12.5% polyacrylamide non-denaturing gel. The gel was then stained for 30 minutes with Redsafe nucleic acid staining solution (iNtRON; Biotechnology, Inc., Toronto, ON, Canada).

UVA and H_2O_2 Exposure and Cell Viability Analysis

Corneal endothelial cells were cultured in 96-well plates until full confluence. For UVA irradiation, cells were washed twice with PBS (Wisent) and covered with phosphate-buffered saline for irradiation with a UVA lamp emitting UVA1 wavelengths (340–400 nm) with <0.01% of UVA2 wavelengths (315–340 nm; UVP 365 nm lamp with filter; UVP, Upland, CA, USA). Cells were irradiated with 0, 100, 200, 300, 400, 500, or 600 kJ/m^2 of UVA and then incubated for 24 hours.

For H_2O_2 experiments, cells were incubated for 24 hours in the presence of H_2O_2 at concentrations of 0, 200, 400, 600, 800, and 1000 μM in culture medium at 37°C and 8% CO_2. Cell viability was then assessed using the Live/Dead viability/cytotoxicity kit for mammalian cells (Life Technologies) according to the manufacturer's protocol. Briefly, cells were washed twice with phosphate-buffered saline and incubated in phosphate-buffered saline with 4 mM calcein AM and 2 mM ethidium homodimer-1 for 35 minutes in the dark at room temperature. They were washed again with phosphate-buffered saline and observed. Signal quantification was done with the AxioVision version 4.8.2 software (Zeiss, Germany). For normalization, the average number of viable cells per field in the control sample (i.e., 0 kJ/m^2 or 0 μM H_2O_2) was set as the baseline for 100% viability. Subsequent conditions were reported as the ratio of number of viable cells per field-to-number of viable cells per field in the control. At least 8 fields were analyzed for each H_2O_2 concentration and UVA dose.

Gene Profiling Analysis

Gene profiling was performed as previously described.[32] Cells from healthy donors and FECD patients were cultured for 24 days post confluence, with the addition of hydrocortisone (0.4 μg/ml; Calbiochem) during the last 7 days. RNA was isolated from the samples using TRizol reagent according to the manufacturer's protocol (Ambion; Life Technologies). Cyanine 3-CTP (Agilent protocol)-labeled cRNA targets were prepared from 200 ng of total RNA from the different samples using the One-Color microarray-based gene expression analysis kit (Agilent Technologies). cRNA (600 ng) was then incubated on a G4851A SurePrint G3 human Ge 8× 60 K array slide (60,000 probes; Agilent Technologies). Slides were hybridized for 18 hours, washed, and scanned using a SureScan scanner (Agilent), and heat maps were analyzed for selected genes using Arraystar version 4.1 software (DNAstar, Madison, WI, USA).

Statistical Analysis

KaleidaGraph version 4.1.3 software (Synergy Software, Reading, PA, USA) was used to generate statistical analysis. Wilcoxon test was used to compare the mtDNA, mtDNA^{CD4977}, and T:S Q-PCR ratio levels of the different samples. Wilcoxon is a nonparametric statistical hypothesis test for paired samples or repeated measurements from a single sample. Box plots and median values illustrate data.[13] Statistical analyses for the microarray experiment were performed using the robust

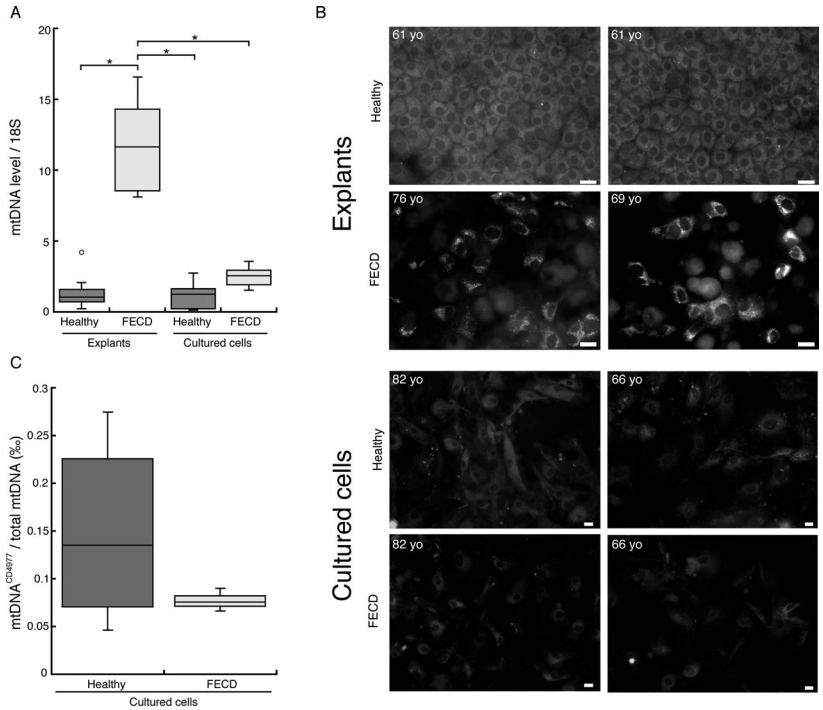

Figure 1. Mitochondrial level and integrity in healthy and FECD corneal endothelium explants and cultured cells. (**A**) The amount of mtDNA per cell was measured using a ratio of the mtDNA level to a known number of copies per cell gene (i.e., gene coding for 18S ribosomal subunit). The mtDNA-to-18S ratio was significantly higher in FECD explants (median: 11.63) than in healthy explants (median: 1.06), healthy cultured cells (median: 1.23), and FECD cultured cells (median: 2.57; $^*P < 0.01$). ($n = 23$ subjects; $n = 5$ experimental repeats per subject; median 67 years of age). (**B**) Mitochondrial density was assessed using Mitotracker Red CMXRos. Corneal endothelial cell mitochondria were found in greater numbers in FECD explants than in healthy explants, healthy cultured cells, and FECD cultured cells. The mitochondrial signal in FECD explants was unevenly distributed; some cells (≈20%–30%) showed a much stronger signal than others. Mitochondrial signal distribution was otherwise uniform and similar among other groups. ($n = 8$ samples; median age: 67.5 years). *White scale bar*: 50 μm. (**C**) Quantification of $mtDNA^{CD4977}$ in FECD and healthy cultured corneal endothelial cells. $mtDNA^{CD4977}$ and total mtDNA were detected by Q-PCR. Total DNA, including mtDNA, was extracted from confluent cultures at passage 3. Specific primer sets were used for $mtDNA^{CD4977}$ and mtDNA detection, and the $mtDNA^{CD4977}$-to-total mtDNA ratio was derived. No significant differences in $mtDNA^{CD4977}$-to-total mtDNA ratio were found between the two conditions; median values of 0.07% and 0.13% for healthy and FECD, respectively. ($n = 8$ subjects; $n = 4$ experimental repeats per subject; median age: 66 years).

multiarray analysis for background correction of the raw data values. Microarray data shown in this study comply with the Minimum Information About a Microarray Experiment (MIAME) requirements.[33]

Results

Differences Between Levels of mtDNA in Healthy and FECD Explants and Cultured Corneal Endothelial Cells and Those of $mtDNA^{CD4977}$

Figure 1A illustrates the amount of mtDNA per corneal endothelial cell as expressed by the ratio total mtDNA molecules-to-total ribosomal 18S subunit DNA sequences (mtDNA:18S). The amount of mtDNA per cell was found to be 11 times higher in FECD explants (median: 11.63) than in healthy explants (median: 1.06). It was also significantly higher in FECD explants (median: 11.63) than in FECD cultured cells (median: 2.57) No significant differences were found between healthy explants, healthy cultured cells (median: 1.23) and FECD cultured cells.

These findings were qualitatively confirmed by mitochondrial staining using Mitotracker dye. The mitochondrial signal was stronger in FECD explants than in healthy explants, healthy cultured cells, and FECD cultured cells. The mitochondrial signal was also unevenly distributed in FECD explants, some cells (≈20%–30%) clearly showed a stronger signal, whereas a uniform distribution was observed in healthy explants, healthy cultured cells, and FECD cultured cells (Fig. 1B).

Figure 1C illustrates the level of mtDNA detected per mitochondrial genome expressed in terms of "mtDNA molecules containing the common deletion/total mtDNA molecules ($mtDNA^{CD4977}$:total mtDNA). No significant accumulation of $mtDNA^{CD4977}$ was seen in FECD cultured cells, as documented by the similar $mtDNA^{CD4977}$:total mtDNA ratios found in healthy (0.07%) and FECD (0.13%) cells in culture (Fig. 1C).

Telomeres Are Shorter in FECD Patients, but Cultured Corneal Endothelial Cells From Healthy and FECD Subjects Showed an Increased Telomere Length Without Telomerase Gene Expression and Activity

Telomeres in cultured cells (relative telomere length T:S for healthy: 12.6, and FECD: 13.7) were significantly longer than in those in the explants (T:S healthy: 4.4 and FECD: 0.9) (Fig. 2A). Notably, telomeres in FECD explants were significantly shorter than telomeres from healthy explants, a difference that was not observed in culture.

As the increase in telomere length observed in cultured cells could be explained either by an increase in telomerase activity or by the selection in culture of cells with longer telomeres, the two options were evaluated. To assess telomerase activity, we first analyzed gene expression of the

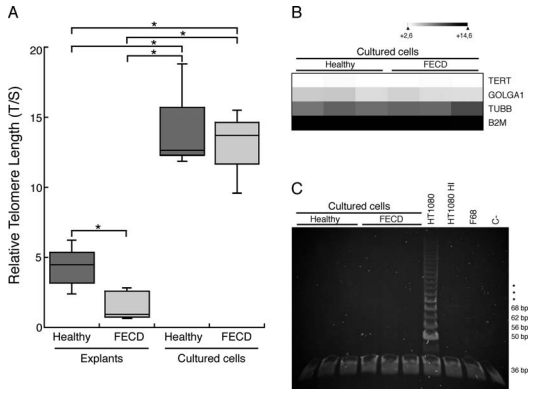

Figure 2. Telomeres are shorter in FECD patients, but cultured corneal endothelial cells from healthy and FECD subjects show an increased telomere length without telomerase gene expression and activity. (**A**) Relative telomere length was evaluated by Q-PCR in corneal endothelium explants and cultured cells from healthy and FECD subjects. Total DNA, including mtDNA, was extracted from explants and from confluent cultured cells at passage 3. The ratio of telomeric Q-PCR amplification signal (T)-to-the signal generated by the single-copy gene HBG (S) was determined (T:S). Relative telomere length was greater in cultured cells (healthy: T:S = 12.6, and FECD: T:S = 13.7) than in explants (Healthy: T:S = 4.4, and FECD: T:S = 0.9). The relative telomere length was significantly less for FECD explants than for healthy explants. (*$P < 0.04$; $n = 17$ subjects; median age: 69 years). (**B**) Gene expression of telomerase-coding gene (TERT) in postconfluent corneal endothelial cultured cells from healthy and FECD subjects using gene expression microarray technique. The scale used to display the log2 expression level values was determined by the hierarchical clustering algorithm of the Euclidian metric distance between genes. *White* indicates a very low and *black* a very high gene expression level. The three genes shown in the *lower lines* (GOLGA1, TUBB, and B2M) are housekeeping genes used as experimental controls, with stable transcription level, independent of cell type and conditions. Results indicate a similar absence of TERT gene expression in healthy and FECD cultured cells. ($n = 6$ subjects; 3 healthy (60, 66 and 82 years old) and 3 FECD subjects (58, 66 and 82 years old); median age: 66 years). (**C**) Telomerase activity measured in cultured corneal endothelial cell from healthy and FECD subjects using the TRAP assay. ($n = 6$; 3 healthy; age, 64, 70, and 72 years old) and 3 FECD (69, 69, and 70 years old; subjects median age: 69.5 years). HT1080 is a telomerase-positive fibrosarcoma cell line, and HT1080 HI is the heat-inactivated control. F68 is a 68-year-old telomerase-negative corneal stromal keratocyte strain, and C– is a negative control without protein extract. The 36-bp fragment is an internal PCR amplification control band. No telomerase activity was found in either type of cultured cells, healthy or FECD.

telomerase-coding gene (TERT) in healthy and FECD cultured cells and found that it was absent in both cases (Fig. 2B). Telomerase activity was then verified using the TRAP assay, which clearly confirmed the absence of telomerase activity in healthy and FECD cultured cells (Fig. 2C). Cells from HT1080, a fibrosarcoma cell line known to express telomerase, were used as positive controls, and normal human corneal stromal diploid keratocytes, known not to express telomerase, were used as negative controls.[34]

Cultured Corneal Endothelial Cell From Healthy and FECD Subjects Are Equally Sensitive to UVA- and H_2O_2-Induced Cell Death

Sensitivities to UVA- and H_2O_2-induced cell death were similar in FECD and healthy cultured endothelial cells, with one exception. FECD cells were more resistant to H_2O_2-induced cell death than healthy cells at a concentration of 1000 μM ($P < 0.05$) (Fig. 3A).

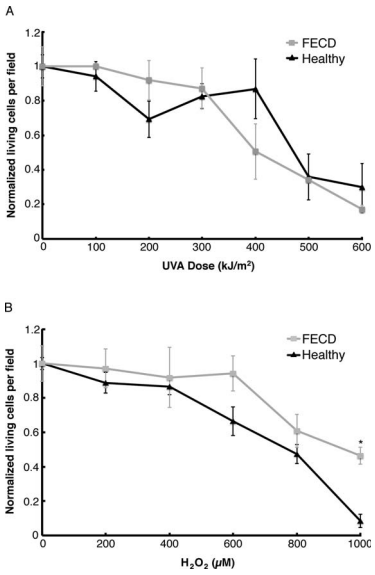

Figure 3. Similar sensitivity to UVA- and H_2O_2-induced mortality in cultured FECD and healthy corneal endothelial cells. (**A**) Cells were irradiated with UVA doses ranging from 0 to 600 kJ/m^2. Cell viability was measured 24 hours after irradiation. The results show no significant differences in UVA-induced cell death sensitivity between cultured corneal endothelial cells from healthy and FECD subjects. Data are means ± SD. ($n = 7$; $n \geq 3$ subjects per condition; median age: 72 years). (**B**) Cells were exposed to H_2O_2 doses ranging from 0 to 1000 μM. Cell viability was measured 24 hours later. No significant differences in H_2O_2-induced cell death were observed between healthy and FECD cells from 0 to 800 μM. In fact, FECD cells seemed to be less susceptible to H_2O_2-induced cell death, and FECD cells exposed to 1000 μM were significantly more resistant to H_2O_2-induced cell death than healthy cells (*$P < 0.05$). Data are means ± SD ($n = 7$; median age: 72 years).

Expression of Genes Implicated in Oxidative Stress Response Is Similar to That in Cultured Corneal Endothelial Cells From Healthy and FECD Subjects

It has been previously shown that genes implicated in antioxidant protection, ROS metabolism, apoptosis, and signaling in response to oxidative stress are deregulated in corneal endothelial cells of FECD patients' explants (Table 3). Gene expression analysis in cultured endothelial cells from healthy and FECD subjects showed no deregulation in the expression of genes implicated in antioxidant protection, ROS metabolism, apoptosis, and signaling in response to oxidative stress (Table 3). The only exception was the transcript level of peroxiredoxin 6 that was found to be significantly up-regulated in cultured FECD cells compared to healthy cells.

Discussion

Increased mtDNA and mtDNA^{CD4977} Levels in Healthy and FECD Corneal Endothelium Explants and Cultured Cells

Increases in cell mitochondria content have been associated with multiple diseases, including breast cancer, hepatitis C virus infection, and chronic obstructive pulmonary disease.[35–38] The increase was described as a compensatory mechanism against defects in mitochondria harboring mutated mtDNA and/or a defective respiratory system and an early cellular response to oxidative stress.[36,39] An abnormal accumulation of mitochondria was documented in a mouse model

Table 3. Comparative List of Genes More Than Two-Fold Down- or Up-Regulated in FECD Explants and Cultured Cells Relative to Normal, as Detected by PCR Array and Gene Profiling

		Explants*	Cultured Cells†
Gene Description	**Symbol**	**Fold Regulation**	**Fold Regulation**
Antioxidant			
Metallothionein 3	*MT3*	−5.65	1.346
Superoxide dismutase 3. extracellular	*SOD3*	−5.37	1.802
Peroxiredoxin 1	*PRDX1*	−2.02	−1.026
Peroxiredoxin 2	*PRDX2*	−4.3	−1.236
Peroxiredoxin 5	*PRDX5*	−3.05	1.311
Peroxiredoxin 6	*PRDX6*	−3.29	2.663
Superoxide dismutase 2. mitochondrial	*SOD2*	−2.65	−1.147
Cytoglobin	*CYGB*	−2.23	−1.558
Thioredoxin reductase 1	*TXNRD1*	−2.23	1.06
Albumin	*ALB*	3.34	−1.135
ROS metabolism			
Neutrophil cytosolic factor 2	*NCF2*	3.48	1.209
Nitric oxide synthase 2A (inductible. hepatocytes)	*NOS2A*	−3.91	1.131
Arachidonate 12-lipoxygenase	*ALOX12*	−2.31	−1.059
Apoptosis			
BCL2/adenovirus E1B 19 kD-interacting protein 3	*BNIP3*	−4.61	−1.027
Glyceraldehyde-3-phosphate dehydrogenase	*GAPDH*	−2.61	−1.088
Signaling in response to oxidative stress			
Dual specificity phosphatase 1	*DUSP1*	−3.12	−1.057
Oxidative-stress response 1	*OXSR1*	−2.18	−1.708
Serine/threonine kinase 25 (STE20 homolog. yeast)	*STK25*	−2.16	1.119
Other oxidative stress responsive genes			
Angiopoietin-like 7	*ANGPTL7*	−4.74	−1.824
Selenoprotein P. plasma. 1	*SEPP1*	−2.03	1.072

* Derived by PCR array analysis. Explants data reprinted with permission from Jurkunas UV, Bitar MS, Funaki T, Azizi B. Evidence of oxidative stress in the pathogenesis of Fuchs' endothelial corneal dystrophy. *Am J Pathol*. 2010;177:2278–2289.

† Derived by gene profiling analysis.

of FECD (Col8a2 knock-in).[40] In the present study, we documented increased levels of mitochondria and mtDNA content in FECD explants (Fig. 1), two parameters that usually correlate. Corneal endothelial cell counts, on the other hand, are known to progressively decline in FECD. We thus hypothesize that the surviving endothelial cells may have to increase their mitochondrial content to produce the ATP needed by the Na/K ATPase ion pump in order to maintain corneal stromal deturgescence. This, in turns, leads to an increase in ROS production by the mitochondrial respiratory chain, and ROS are known to catalyze the apparition of mtDNA deletion, such as the mtDNA^{CD4977}.[41,42] In accordance with this hypothesis, Czarny et al.[43] recently documented an increase in the number of mtDNA copies and mtDNA^{CD4977} in the corneal endothelium of FECD patients compared with healthy subjects. Because mtDNA accumulates with age,[36,39] FECD and healthy groups were matched for age in this study.

We then showed that culturing FECD cells restores a normal phenotype in terms of mitochondria and mtDNA content (Fig. 1). Using Mitotracker dye, we found that the mitochondrial signal was uneven in FECD explants, with 20% to 30% of the cells showing a much stronger signal (Fig. 1B). This may indicate that these high mitochondria-containing cells were highly active and produced more ROS, which in turn would further exacerbate the oxidative damage and lead to an increase in mtDNA deletions.[3,9,10,23,43] Increased levels of mitochondrial ROS have indeed been documented in FECD cells.[12] Beyond a certain threshold, increased ROS levels induce release of mitochondrial cytochrome c, leading to apoptosis.[39] This may explain in part endothelial cell attrition in FECD.

Czarny et al.[43] also documented an increase in occurrence of mtDNA^{CD4977} in FECD corneal endothelium explants compared with that in healthy explants. We found no significant differences in mtDNA^{CD4977} levels between healthy (0.07%) and FECD (0.13%) and healthy cultured endothelial cells (Fig. 1). Notably, a similar percentage has been reported for normal endothelial explants (0.13%),[14] supporting hypotheses of either a rehabilitation by culture or the selection of cells containing less deletion.

Relative Telomere Length, Telomerase Gene Expression, and Telomerase Activity in Isolated Corneal Endothelial Cells From FECD

Telomeres were 4 times shorter in FECD explants than in healthy explants (Fig. 2A). DNA telomeric repeats stabilize chromosomes and help preserve genome integrity. Telomeric DNA, however, is highly sensitive to oxidative damage, which causes telomeric shortening and accelerates cellular senescence and cell death.[15,44] Because of the significant role of oxidative stress in FECD, we investigated telomere lengths in corneal endothelial cells from FECD and from healthy subjects. Once telomere erosion reaches a certain threshold, the cell enters a senescent state or exhibits chromosomic aberrations.[45]

Our results also showed that telomeres in cultured cells (healthy and FECD) were significantly longer than telomeres

from explants (healthy and FECD). The fact that no telomerase (hTERT) gene expression and no telomerase activity could not be detected in either healthy or FECD cultured cells (Fig. 2) strongly favors the hypothesis of a selection in culture of cells with longer telomeres, whether these are healthy or FECD cells.

No Difference in UVA- and H_2O_2-Induced Cell Death Sensitivity and in Gene Implicated in Oxidative Stress Response Between Cultured Endothelial Cells From Healthy and FECD Subjects

FECD cells are poorly protected against oxidative stress, and they are exposed to both endogenous (mitochondrial respiratory chain) and exogenous oxidation (UVA) throughout life, which makes them prone to cell death.[9,10,46,47] UVA wavelengths were used in this experiment because they represent 75% of the terrestrial UV radiations, they are known to reach the corneal endothelium, and they efficiently induce ROS.[6–8,48] H_2O_2, an oxidizing component induced by the mitochondrial respiratory chain, was also used to assess sensitivity to oxidative stress. Both UVA- and H_2O_2-induced cell death methods showed that FECD and healthy cultured cells behave similarly in the presence of oxidative stress (Fig. 3). FECD cells seemed slightly less sensitive than healthy cells, but this was only statistically significant for the highest concentration (1000 μM).

The similarity between FECD and healthy cultured cells was further confirmed by gene profiling results showing that major genes implicated in antioxidant protection, ROS metabolism, apoptosis, and signaling in response to oxidative stress were not deregulated (i.e., were less than 2-fold down- or up-regulated) in FECD cultured cells, with the only exception being peroxiredoxin 6 upregulation (Table 3). Peroxiredoxin 6 is a cytoprotective antioxidant enzyme working against endogenous or exogenous peroxide, widely expressed in tissues.[49] Although interesting, investigation of its role in FECD was beyond the purpose of this study. As shown in Table 3, we did not find a gene deregulation similar to that reported in explants of FECD corneal endothelium in cultured cells.[10] Overall, these results converge to highlight the fact that endothelial cell culture allows rehabilitation of the oxidant-antioxidant balance in FECD.

In this study, we showed that late stage FECD corneal endothelium contains cells that are comparable to healthy endothelial cells in terms of mitochondrial amount and integrity, telomere length, sensitivity to oxidation, and oxidant-antioxidant gene expression. We also showed that these functional cells could be selected and amplified by cell culture. This could explain previous results showing that an endothelium tissue-engineered using cultured corneal endothelial cells from patients with end-stage FECD cells retains some functionality.[24] Currently, the only treatment for FECD is transplantation of an allogeneic corneal endothelium, using donor tissue. This work opens the door to a new therapeutic concept, where rehabilitation of a diseased FECD endothelium could potentially be achieved through reimplantation of a new corneal endothelium tissue engineered from cultured autologous endothelial cells.

Acknowledgments

The authors thank Banque d'Yeux du Centre Universitaire d'Ophtalmologie de Québec for providing the donor corneas and Banque Québécoise de Cellules Cornéennes for providing the FECD corneal endothelial cells. The authors also thank Richard Bazin, Isabelle Brunette, Patrick-Ann Laughrea, Marie-Eve Légaré, and Julia Talajic for providing FECD corneal endothelium explants.

Supported by Canadian Institutes of Health Research grant (IB, SP, PJR), Fonds de Recherche du Québec-Santé (research scholars PJR and SP), and FRQ-S Doctoral Research Award (SPG), and the Quebec Eye Tissue Bank for Vision Research is partly supported by the FRQ-S Vision Health Research Network.

Disclosure: **S.P. Gendron**, None; **M. Thériault**, None; **S. Proulx**, None; **I. Brunette**, None; **P.J. Rochette**, None

References

1. Musch DC, Niziol LM, Stein JD, Kamyar RM, Sugar A. Prevalence of corneal dystrophies in the United States: estimates from claims data. *Invest Ophthalmol Vis Sci*. 2011; 52:6959–6963.
2. Hamill CE, Schmedt T, Jurkunas U. Fuchs endothelial cornea dystrophy: a review of the genetics behind disease development. *Semin Ophthalmol*. 2013;28:281–286.
3. Schmedt T, Silva MM, Ziaei A, Jurkunas U. Molecular bases of corneal endothelial dystrophies. *Exp Eye Res*. 2012;95:24–34.
4. Zhang J, Patel DV. The pathophysiology of Fuchs' endothelial dystrophy—a review of molecular and cellular insights. *Exp Eye Res*. 2015;130:97–105.
5. Bonanno JA. Molecular mechanisms underlying the corneal endothelial pump. *Exp Eye Res*. 2011;95:2–7.
6. Mallet JD, Rochette PJ. Ultraviolet light-induced cyclobutane pyrimidine dimers in rabbit eyes. *Photochem Photobiol*. 2011; 87:1363–1368.
7. Mallet JD, Rochette PJ. Wavelength-dependent ultraviolet induction of cyclobutane pyrimidine dimers in the human cornea. *Photochem Photobiol*. 2013;12:1310–1318.
8. Cadet J, Douki T, Ravanat JL. Oxidatively generated damage to cellular DNA by UVB and UVA radiation. *Photochem Photobiol*. 2015;91:140–155.
9. Liu C, Chen Y, Kochevar IE, Jurkunas UV. Decreased DJ-1 leads to impaired Nrf2-regulated antioxidant defense and increased UV-A-induced apoptosis in corneal endothelial cells. *Invest Ophthalmol Vis Sci*. 2014;55:5551–5560.
10. Jurkunas UV, Bitar MS, Funaki T, Azizi B. Evidence of oxidative stress in the pathogenesis of fuchs endothelial corneal dystrophy. *Am J Pathol*. 2010;177:2278–2289.
11. Johns DR. Seminars in medicine of the Beth Israel Hospital, Boston. Mitochondrial DNA and disease. *N Engl J Med*. 1995; 333:638–644.
12. Elhalis H, Azizi B, Jurkunas UV. Fuch's endothelial corneal dystrophy. *Ocul Surf*. 2010;8:173–184.
13. Gendron SP, Bastien N, Mallet JD, Rochette PJ. The 3895-bp mitochondrial DNA deletion in the human eye: a potential involvement in corneal ageing and macular degeneration. *Mutagenesis*. 2013;28:197–204.
14. Gendron SP, Mallet JD, Bastien N, Rochette PJ. Mitochondrial DNA common deletion in the human eye: a relation with corneal aging. *Mech Ageing Dev*. 2012;133:68–74.
15. Pawlas N, Plachetka A, Kozlowska A, et al. Telomere length, telomerase expression and oxidative stress in lead smelters. *Toxicol Ind Health* 2015.
16. Tchirkov A, Lansdorp PM. Role of oxidative stress in telomere shortening in cultured fibroblasts from normal individuals and patients with ataxia-telangiectasia. *Hum Mol Genet*. 2003;12: 227–232.
17. von Zglinicki T. Oxidative stress shortens telomeres. *Trends Biochem Sci*. 2002;27:339–344.
18. Bitar MS, Liu C, Ziaei A, Chen Y, Schmedt T, Jurkunas UV. Decline in DJ-1 and decreased nuclear translocation of Nrf2 in Fuch's endothelial corneal dystrophy. *Invest Ophthalmol Vis Sci*. 2012;53:5806–5813.
19. Azizi B, Ziaei A, Fuchsluger T, Schmedt T, Chen Y, Jurkunas UV. p53-regulated increase in oxidative-stress—induced apoptosis

in Fuchs endothelial corneal dystrophy: a native tissue model. *Invest Ophthalmol Vis Sci*. 2011;52:9291–9297.

20. Gottsch JD, Bowers AL, Margulies EH, et al. Serial analysis of gene expression in the corneal endothelium of Fuchs' dystrophy. *Invest Ophthalmol Vis Sci*. 2003;44:594–599.
21. Buddi R, Lin B, Atilano SR, Zorapapel NC, Kenney MC, Brown DJ. Evidence of oxidative stress in human corneal diseases. *J Histochem Cytochem*. 2002;50:341–351.
22. Wang Z, Handa JT, Green WR, Stark WJ, Weinberg RS, Jun AS. Advanced glycation end products and receptors in Fuchs' dystrophy corneas undergoing Descemet's stripping with endothelial keratoplasty. *Ophthalmology*. 2007;114:1453–1460.
23. Jurkunas UV, Rawe I, Bitar MS, et al. Decreased expression of peroxiredoxins in Fuchs' endothelial dystrophy. *Invest Ophthalmol Vis Sci*. 2008;49:2956–2963.
24. Haydari MN, Perron MC, Laprise S, et al. A short-term in vivo experimental model for Fuchs endothelial corneal dystrophy. *Invest Ophthalmol Vis Sci*. 2012;53:6343–6354.
25. Zaniolo K, Bostan C, Rochette Drouin O, et al. Culture of human corneal endothelial cells isolated from corneas with Fuchs endothelial corneal dystrophy. *Exp Eye Res*. 2012;94:22–31.
26. Zhu C, Joyce NC. Proliferative response of corneal endothelial cells from young and older donors. *Invest Ophthalmol Vis Sci*. 2004;45:1743–1751.
27. Proulx S, Bourget JM, Gagnon N, et al. Optimization of culture conditions for porcine corneal endothelial cells. *Mol Vis*. 2007;13:524–533.
28. Karabekian Z, Gillum ND, Wong EW, Sarvazyan N. Effects of N-cadherin overexpression on the adhesion properties of embryonic stem cells. *Cell Adh Migr*. 2009;3:305–310.
29. Aviv A, Hunt SC, Lin J, Cao X, Kimura M, Blackburn E. Impartial comparative analysis of measurement of leukocyte telomere length/DNA content by Southern blots and qPCR. *Nucleic Acids Res*. 2011;39:e134.
30. O'Callaghan NJ, Fenech M. A quantitative PCR method for measuring absolute telomere length. *Biol Proced Online*. 2011;13:3.
31. Rochette PJ, Brash DE. Human telomeres are hypersensitive to UV-induced DNA Damage and refractory to repair. *PLoS Genetics*. 2010;6:e1000926.
32. Gendron SP, Rochette PJ. Modifications in stromal extracellular matrix of aged corneas can be induced by ultraviolet A irradiation. *Aging Cell*. 2015;14:433–442.
33. Brazma A, Hingamp P, Quackenbush J, et al. Minimum information about a microarray experiment (MIAME)-toward standards for microarray data. *Nat Genet*. 2001;29:365–371.
34. Hsu CC, Chen CH, Hsu TI, et al. The 58-kDa microspherule protein (MSP58) represses human telomerase reverse transcriptase (hTERT) gene expression and cell proliferation by interacting with telomerase transcriptional element-interacting factor (TEIF). *Biochim Biophys Acta*. 2014;1843:565–579.
35. Hsu CW, Yin PH, Lee HC, Chi CW, Tseng LM. Mitochondrial DNA content as a potential marker to predict response to anthracycline in breast cancer patients. *Breast J*. 2010;16:264–270.
36. Lee HC, Yin PH, Lu CY, Chi CW, Wei YH. Increase of mitochondria and mitochondrial DNA in response to oxidative stress in human cells. *Biochem J*. 2000;348(Pt 2):425–432.
37. Liu SF, Kuo HC, Tseng CW, et al. Leukocyte mitochondrial DNA copy number is associated with chronic obstructive pulmonary disease. *PLoS One*. 2015;10:e0138716.
38. Zhang AM, Ma K, Song Y, et al. Mitochondrial DNAs decreased and correlated with clinical features in HCV patients from Yunnan, China. *Mitochondrial DNA*. 2016;27:2516–2519.
39. Lee HC, Wei YH. Mitochondrial role in life and death of the cell. *J Biomed Sci*. 2000;7:2–15.
40. Meng H, Matthaei M, Ramanan N, et al. L450W and Q455K Col8a2 knock-in mouse models of Fuchs endothelial corneal dystrophy show distinct phenotypes and evidence for altered autophagy. *Invest Ophthalmol Vis Sci*. 2013;54:1887–1897.
41. Berneburg M, Grether-Beck S, Kurten V, et al. Singlet oxygen mediates the UVA-induced generation of the photoaging-associated mitochondrial common deletion. *J Biol Chem*. 1999;274:15345–15349.
42. Krishnan KJ, Harbottle A, Birch-Machin MA. The use of a 3895 bp mitochondrial DNA deletion as a marker for sunlight exposure in human skin. *J Invest Dermatol*. 2004;123:1020–1024.
43. Czarny P, Seda A, Wielgorski M, et al. Mutagenesis of mitochondrial DNA in Fuchs endothelial corneal dystrophy. *Mutat Res*. 2014;760:42–47.
44. Li H, Hedmer M, Wojdacz T, et al. Oxidative stress, telomere shortening, and DNA methylation in relation to low-to-moderate occupational exposure to welding fumes. *Environ Mol Mutagen*. 2015;56:684–693.
45. Capper R, Britt-Compton B, Tankimanova M, et al. The nature of telomere fusion and a definition of the critical telomere length in human cells. *Genes Dev*. 2007;21:2495–2508.
46. Eghrari AO, Gottsch JD. Fuchs' corneal dystrophy. *Expert Rev Ophthalmol*. 2010;5:147–159.
47. Wojcik KA, Kaminska A, Blasiak J, Szaflik J, Szaflik JP. Oxidative stress in the pathogenesis of keratoconus and Fuchs endothelial corneal dystrophy. *Int J Mol Sci*. 2013;14:19294–19308.
48. Tewari A, Grys K, Kollet J, Sarkany R, Young AR. Upregulation of MMP12 and its activity by UVA1 in human skin: potential implications for photoaging. *J Invest Dermatol*. 2014;134:2598–2609.
49. Knoops B, Goemaere J, Van der Eecken V, Declercq JP. Peroxiredoxin 5: structure, mechanism, and function of the mammalian atypical 2-Cys peroxiredoxin. *Antioxid Redox Signal*. 2011;15:817–829.

Investigative Ophthalmology & Visual Science